Brief Communication

Mutations in AMPA receptor-associated *FRRS1L* lead to a hyperkinetic movement disorder in mice and humans

Marianna Madeo[1*], Michelle Stewart[2*], Yuyang Sun[3], Nadia Sahir[1], Sarah Wiethoff[4], Indra Chandrasekar[1], Anna Yarrow[1], Jill A Mokry[5], Yaping Yang[5], Dawn Cordeiro[6], Elizabeth M McCormick[7], Colleen C Murarescu[7], Tyler N. Jepperson[1], Lauren McBeth[1], Mohammed Zain Seidahmed[8], Heba El Khashab[9,10], Muddathir Hamad[9], Hamid Azzedine[11], Karl Clark[12], Silvia Corrochano[2], Sara Wells[2], Mariet W Elting[13], Marjan M Weiss[13], Sabrina Burn[1], Angela Myers[1], Megan Landsverk[1], Patricia L Crotwell[1], Quinten Waisfisz[13], Nicole I. Wolf[14], Patrick M. Nolan[2], Sergio Padilla-Lopez[15,16], Henry Houlden[4], Richard Lifton[17], Shrikant Mane[17], Brij Singh[3], Marni Falk[7*], Saadet Mercimek-Mahmutoglu[6*], Mustafa A. Salih[9*], Kaya Bilguvar[17*], Abraham Acevedo-Arozena[2*], Michael C. Kruer[1,15,16,18,19*#]

1 Children's Health Research Center, Sanford Research
Sioux Falls, SD 57104 USA

2 MRC Harwell, Mammalian Genetics Unit
Oxfordshire, OX11 ORD, UK

3 Department of Basic Sciences
University of North Dakota
Grand Forks, ND 58202 USA

4 Department of Molecular Neuroscience, Lila Reta Weston Institute of Neurology, University College London
London WC1H 0AJ UK

5 Department of Molecular & Human Genetics, Baylor College of Medicine
Houston, TX, 77030 USA

6 Department of Pediatrics, Division of Clinical & Metabolic Genetics and Genetics & Genome Biology Program, The Hospital for Sick Children, University of Toronto
Toronto, Ontario, M5G 1X8 Canada

7 Department of Pediatrics, Division of Human Genetics and Division of Child Development & Metabolic Disease, The Children's Hospital of Philadelphia
Philadelphia, PA, 19104 USA

8 Department of Pediatrics, Security Forces Hospital
Riyadh, 12625 Saudi Arabia

9 Department of Pediatrics, Division of Pediatric Neurology, College of Medicine, King Saud University
Riyadh, 12372 Saudi Arabia

10 Department of Pediatrics, Ain Shams University Hospital
Cairo, 11355 Egypt

11 Institute of Neuropathology, Uniklink-RWTH

Aachen, 52074 Germany

12 Department of Biochemistry and Molecular Biology, Mayo Clinic
Rochester, MN, 55905 USA

13 Department of Clinical Genetics
VU University Medical Center
Amsterdam, 1007 The Netherlands

14 Department of Child Neurology and Neuroscience Campus Amsterdam
VU University Medical Center
Amsterdam, 1007 The Netherlands

15 Department of Child Health, University of Arizona College of Medicine
Phoenix, AZ, 85004 USA

16 Neurogenetics Research Program, Barrow Neurological Institute, Phoenix Children's Hospital, Phoenix, AZ, 85016 USA

17 Yale Genomics Center
New Haven, CT, 06516 USA

18 Program in Neuroscience, Arizona State University
Tempe, AZ, 85287 USA

19 Movement Disorders Center, Barrow Neurological Institute, Phoenix Children's Hospital, Phoenix, AZ, 85016 USA

* These authors contributed equally

Author emails:

Marianna Madeo	marianna.madeo@sanfordhealth.org
Michelle Stewart	m.stewart@har.mrc.ac.uk
Yuyang Sun	yuyang.sun@med.und.edu
Nadia Sahir	nasahir29@gmail.com
Sarah Wiethoff	s.wiethoff.12@ucl.ac.uk
Indra Chandrasekar	indra.chandrasekar@sanfordhealth.org
Anna Yarrow	yarrowa@mymail.vcu.edu
Jill Mokry	jill.mokry@bcm.edu
Yaping Yang	yapingy@bcm.edu
Dawn Cordeiro	dawn.cordeiro@sickkids.ca
Elizabeth McCormick	mccormicke@email.chop.edu
Colleen Murarescu	murarescuc@email.chop.edu
Tyler Jepperson	tyler.jepperson@avera.org
Lauren McBeth	laurenjmcbeth@gmail.com
Mohammed Seidahmed	zainsidahmed@hotmail.com
Heba El Khashab	heba241@hotmail.com
Muddathir Hamad	mudhamad@yahoo.com
Hamid Azzedine	azzedine.hamid@yahoo.fr
Karl Clark	clark.karl@mayo.edu

Silvia Corrochano s.corrochano@har.mrc.ac.uk
Sara Wells s.wells@har.mrc.ac.uk
Mariet Elting m.elting@vumc.nl
Marjan Weiss j.weiss@vumc.nl
Sabrina Burn sabrina.burn@usd.edu
Angela Myers angmyers@stanford.edu
Megan Landsverk megan.landsverk@sanfordhealth.org
Patricia Crotwell patricia.crotwell@sanfordhealth.org
Quinten Waisfisz q.waisfisz@vumc.nl
Nicole Wolf n.wolf@vumc.nl
Pat Nolan p.nolan@har.mrc.ac.uk
Sergio Padilla-Lopez spadillalopez@email.arizona.edu
Henry Houlden h.houlden@ion.ucl.ac.uk
Rick Lifton richard.lifton@yale.edu
Shrikant Mane shrikant.mane@yale.edu
Brij Singh brij.singh@med.und.edu
Marni Falk falkm@email.chop.edu
Saadet Mercimek-Mahmutoglu saadet.mahmutoglu@sickkids.ca
Mustafa Salih mustafa_salih05@yahoo.com
Kaya Bilguvar kaya.bilguvar@yale.edu
Abraham Acevedo-Arozena a.acevedo@har.mrc.ac.uk
Michael Kruer mkruer@phoenixchildrens.com

Correspondence should be addressed to M.C.K. (mkruer@phoenixchildrens.com)

The etiology of many severe childhood movement disorders remains uncharacterized. We describe a novel neurological disorder with prominent hyperkinetic movements in both mice and humans caused by mutations in *FRRS1L*, an AMPA receptor outer core protein. Loss of FRRS1L function attenuates AMPA-mediated currents, implicating chronic abnormalities of glutamatergic neurotransmission in this monogenic neurological disease of childhood.

Pediatric movement disorders encompass a heterogeneous group of neurodevelopmental and neurodegenerative disorders affecting movement and limiting activities of daily living (1). Huntington disease (HD) is a progressive neurodegenerative disease characterized by impairment of volitional movement, chorea and subcortical dementia due to a CAG triplet repeat expansion in *HTT*. Although uncommon, juvenile HD (JHD) represents an important cause of pediatric movement disorders (2). Although the majority of patients with clinical features of HD will ultimately be found to have an expanded *HTT* allele, several phenocopies have been described, yet the cause of most HD-like syndromes remains uncharacterized (3). We set out to identify genes that lead to HD-like phenotypes and enrolled eligible families in our institutional review board and ethics committee-approved studies after informed consent was obtained.

The index family hailed from southern Saudi Arabia, and the parents were distant cousins (**Supplementary Figure 1a)**. All five of the couple's children developed progressive chorea, dementia and epilepsy without expansion of *HTT* (**Supplementary Table 1**). Over time, a rigid, akinetic presentation began to predominate. One child had already succumbed to the disease at the time of ascertainment. All laboratory studies were unrevealing. Brain MRI was initially normal, but repeat neuroimaging demonstrated diffuse cortical and cerebellar volume loss with flattening of the caudate heads (**Supplementary Figure 1b**).

Given the family structure and presumed autosomal recessive nature of the disorder, we then applied tandem homozygosity mapping and whole exome sequencing. We identified six regions of homozygosity >3 Mb shared by affected family members alone (**Supplementary Table 2**). We performed whole exome sequencing on patients 1_II:-1-4 and focused our analysis on homozygous stop-gain, stop-loss, or frameshift and splice-site or missense variants predicted to be deleterious. We excluded variants with a reported minor allele frequency >0.01 based on ExAc Browser and Exome Variant Server databases. Using this strategy, we identified a homozygous c.961C>T (p.G321*) mutation in *FRRS1L* (aka *c9orf4*) (NM_014334) within a prominent block of homozygosity (hg19; chr9:104,622,396-119,149,440). We confirmed segregation within affected family members by Sanger sequencing (**Supplementary Figure 1a**). This mutation has not been reported in variation repositories, and is predicted to lead to loss of a C-terminal hydrophobic motif that may contribute to FRRS1L's membrane localization (**Figure 1a**).

We subsequently identified three additional, unrelated patients with similar phenotypes (**Supplemental Video 1**) by whole exome sequencing [patient 2_II-1: homozygous c.845G>A (p.W282*)]; patient 3_II-1: homozygous c.737_739del (p.G246del)]; patient 4_II-2 c.436dup; (p.Ile146Asnfs*10) (**Supplementary Table 1**) and confirmed mutations by Sanger sequencing (**Supplementary Figure 1a**). None of these variants has been identified in public repositories. Targeted sequencing of *FRRS1L* in a cohort of 52 pediatric and adult patients with an early-onset Huntington-like phenotype but without demonstrable mutations in *HTT* did not reveal any putatively pathogenic biallelic mutations (**Supplementary Table 3**). Additionally, no biallelic *FRRS1L* mutations were detected in the Epi4K and EuroEPINOMICS RES epilepsy consortia datasets.

Using patient fibroblasts and age and sex-matched controls, we next performed RT-PCR to determine whether the c.961C>T and c.845G>A mRNAs are subject to nonsense-mediated decay. Although *FRRS1L* is predominantly expressed in the brain (**Supplementary Figure 2a**), it is expressed at a lower level in fibroblasts (4) (**Figure 1b**). For both c.961C>T and c.845G>A, consistent with a mutation location near the 3' end of the transcript, we found equal levels of both control and mutant transcripts (**Supplementary Figure 2b**). Both the (p.G321*) and

(p.W282*) patient fibroblasts exhibited a marked decrease in FRRS1L levels by immunoblot (**Figure 1b**).

Little is known about the biological function of FRRS1L. Despite its name (ferric chelate reductase-like 1), it lacks a ferrochelatase domain, and so is unlikely to function in iron storage and processing. A recent study instead identified FRRS1L as an important component of the outer core of AMPA glutamate receptor accessory proteins (5), suggesting that loss of FRRS1L would affect AMPA receptor constituency and might affect AMPA receptor function. In that study, FRRS1L co-immunoprecipitated with GluR1, suggesting a direct interaction between the two proteins. In order to study the effect(s) of FRRS1L loss of function, we first sought to determine the normal localization of FRRS1L and characterize interactions with AMPA receptors. Using mouse primary neurons, we found high FRRS1L expression at the plasma membrane and in agreement with the prior proteomics study, the protein co-localizes with AMPA receptors on the neuronal surface (**Figure 1c**). However, the identification of widespread GluR1-containing AMPA receptors lacking FRRS1L co-localization suggests that FRRS1L is likely found in only a subset of AMPA receptors. These findings are not surprising, as recent work has highlighted the remarkable molecular diversity of glutamate receptors (6).

We sought to determine whether the loss of the transmembrane-association motif (residues 322-342) would lead to altered localization in (p.G321*) and (p.W282*) patient cells. We found diminished co-localization with AMPA receptors at the cell surface membrane demonstrable by total internal reflectance microscopy (TIRF) (**Figure 1d**).

We next sought to determine how the loss of FRRS1L seen in our patients could affect AMPA receptor function. Using neuronally-differentiated SH5Y-SY cells, we knocked down *FRRS1L* using siRNA, leading to a reduction in FRRS1L levels similar to that seen in patient cells (**Supplementary Figure 3**). We next performed a series of patch-clamp experiments with a focus on AMPA-mediated currents. We found that loss of FRRS1L significantly attenuated calcium influx (**Figure 1e,f**) and diminished AMPA-induced inward currents (**Figure 1g-i**).

In parallel with the human studies, a *Frrs1l* null mouse (*Frrs1l*^{Tm1b}/^{Tm1b}) was generated as part of the International Mouse Phenotyping Consortium by homologous recombination followed by excision of the Neo cassette (**Supplementary Figure 4a**). Loss of *Frrs1l* was confirmed by both sequence analysis and western blot (**Supplementary Figure 4b,c**). Similar to human patients with homozygous mutations, null mice exhibited disordered hyperkinetic movements from a young age (**Supplemental Video 2a,b**).

Phenotypic characterization of *Frrs1l*^{Tm1b}/^{Tm1b} animals revealed both evidence of neuromotor dysfunction (**Figure 2a**) as well as impaired volitional movement (**Figure 2b**). Both of these features are very similar to those observed in human *FRRS1L* patients. Although no spontaneous seizures were observed in *Frrs1l*^{Tm1b}/^{Tm1b} mice, early death occurred (**Figure 2c**), indicating postnatal demise. Necropsy analysis of these animals did not reveal an evident cause of death. Neuropathological analysis of knockout animals at age 16 weeks showed morphologically normal brains (**Supplementary Figure 5**), as seen in early MRIs in human patients.

We next evaluated *Frrs1l* expression in embryos and adult mice using a lacZ reporter. In E12.5 embryos, *Frrs1l* expression was evident in the ventral forebrain but lower level expression was seen in the remainder of the embryo while *Frrs1l* expression was highest in the adult brain in the cortex, cerebellum, hippocampus, and basal ganglia (**Supplementary Figure 2a**). This is consistent with prior reports which indicated robust expression in multiple brain regions, including striatum, thalamus, and cortex (7, 8). Developmentally, Frrs1l may play a role in

neuronal maturation, as AMPA receptors promote the formation and maturation of synapses during development (9).

Our findings implicate FRRS1L as an important modulator of glutamate signaling with substantial implications in health and disease. AMPA receptors mediate fast excitatory postsynaptic potentials (EPSCs) in the human brain. EPSCs in turn are largely mediated by inwardly directed Ca^{2+} currents at the postsynaptic spine. AMPA receptor complexity is only now beginning to be appreciated, as dozens of auxiliary subunits govern ion channel gating properties, and dynamic changes in AMPA receptor composition are likely to affect localization and abundance within the synapse (10-12). FRRS1L is an outer core protein that is thought to function within the AMPA receptor and directly interact with inner core components, as illustrated by the ability to immunoprecipitate FRRS1L after GluR1/2 pull-down (5). The significant diminution of AMPA-mediated currents we observed with *FRRS1L* knockdown points to an important role for the protein in normal AMPA receptor function whose relevance has not previously been appreciated. Our findings suggest that loss-of-function mutations may impair normal glutamatergic neurotransmission, leading to a hyperkinetic movement disorder, epilepsy, and a progressive course related to chronic disruption of normal neuronal circuit function.

Mutations in another AMPA receptor outer core component, *PRRT2*, have been shown to lead to seizures and chorea in affected individuals (13). Patients with mutations in *PRRT2* generally have paroxysmal symptoms rather than a degenerative course, but such cases typically involve heterozygous mutations rather than the homozygous mutation we observed in our cases. The recent identification of patients with biallelic *PRRT2* mutations suggests a more severe phenotype in such individuals (14). The identification of additional patients with mutations in *FRRS1L* or related AMPA receptor core proteins will help shed light on the role of these accessory proteins in modulating glutamatergic signaling in the central nervous system, whose complexities are now beginning to be unraveled (15).

URLs

Superlink Online SNP 1.1 http://cbl-hap.cs.technion.ac.il/superlink-snp/main.php
RefSeq http://www.ensembl.org/index.html
HGVS www.hgvs.org
BWA http://bio-bwa.sourceforge.net
GATK https://www.broadinstitute.org/gatk
PICARD http://picard.sourceforge.net/)
SIFT http://sift.jcvi.org/
Polyphen-2 http://genetics.bwh.harvard.edu/pph2/
Mutation Taster www.mutationtaster.org
Combined Annotation Dependent Depletion http://cadd.gs.washington.edu
Uniprot www.uniprot.org
Phosphosite Plus www.phosphosite.org
dbSNP http://www.ncbi.nlm.nih.gov/SNP/
1000 Genomes Project http://www.1000genomes.org/
Exome Variant Server http://evs.gs.washington.edu/EVS/
Exome Aggregation Consortium (ExAC) http://exac.broadinstitute.org/
International Mouse Phenotyping Consortium www.mousephenotype.org
Mouse Genome Informatics www.informatics.jax.org
ClinVar http://www.ncbi.nlm.nih.gov/clinvar/
FRRS1L mutations have been submitted to ClinVar; accession numbers pending

Methods

Methods and associated references are available in the online version of the manuscript.

Acknowledgments

We thank the patients and their families for their gracious participation in these studies. MRC Harwell is a member of the IMPC and has received funding from the National Institutes for Health for generating (U42OD011174) and/or phenotyping (U54HG006348) the *Frrs1l-tm1b*(EUCOMM)Hmgu mice. The research reported in this publication is solely the responsibility of the authors and does not necessarily represent the official views of the National Institutes of Health. These studies were also supported by the Deanship of Scientific Research, King Saud University, Riyadh, Saudi Arabia (MAS; RGP-VPP-301), by a Sanford Seed Grant (AM, PLC, and MCK), by the NIH Centers for Mendelian Genomics (5U54HG006504) (RL, KB, SM) and a Doris Duke Charitable Foundation Clinical Scientist Development Award (CSDA2014112; MCK).

Author contributions

RL, PMN, KB, SM, AAA and MCK designed the study. MM, MS, YS, NS, SW, IC, AY, LM, TNJ, KC, SB, AM, PLC, SC, SW, HH, SPL, PMN, BS, KB, SM, AAA, and MCK designed and/or performed experiments. MM, MS, YS, NS, SW, IC, AY, SB, PLC, ML, PMN, MWE, MMW, QS, NIW, KB, AAA, and MCK analyzed data. MAS, SMM, DC, EMM, CCM, JAM, YY, MZS, HEK, MH, HA, MF, NIW, and MCK recruited and/or evaluated patients and collected samples. MCK wrote the manuscript. HH, SPL, BS, RL, KB, SM, AAA, and MCK edited the manuscript.

Competing Financial Interests

The authors have nothing to declare.

References

1. Kruer MC. *Pediatr Rev* 36(3):104-116 (2015).
2. Telenius H*, et al. Hum Mol Genet* 2(10):1535-1540 (1993).
3. Hensman Moss DJ*, et al. Neurology* 82(4):292-299 (2014).
4. Dememes D, *et al. Brain Res* 671:83-94 (1995).
5. Schwenk J*, et al. Neuron* 74(4):621-633 (2012).
6. Shanks NF, *et al. Cell Rep*. 1(6):590-8 (2012).
7. Chadwick BP*, et al. Mamm Genome* 11(1):81-83 (2000).
8. Schwenk J, *et al*. *Neuron*. 2014 Oct 1;84(1):41-54.
9. McKinney RA, *et al*. *J Physiol* 588(Pt 1):107-116 (2010).
10. Soto D*, et al. Nat Neurosci* 12(3):277-285 (2009).
11. Tomita S*, et al. Nature* 435(7045):1052-1058 (2005).
12. von Engelhardt J*, et al. Science* 327(5972):1518-1522 (2010).
13. Heron SE*, et al. Am J Hum Genet* 90(1):152-160 (2012).
14. Delcourt M*, et al. J Neurol Neurosurg Psychiatry* (2015).
15. Aoto J, *et al*. *Cell* 154(1):75-88 (2013).

Figure legends

Figure 1: Mutations in human FRRS1L and effects of loss of function on cell biology. (**a**) The two premature truncation codon mutations are predicted to lead to loss of the FRRS1L transmembrane domain. (**b**) Immunoblot in patient fibroblasts demonstrates diminished levels of FRRS1L in both patients with premature stop mutations compared to age and sex-matched controls (representative image). (**c**) FRRS1L expression in wild-type primary mouse neurons; a high degree of co-localization with GluR1 is seen (Pearson's r= 0.70). (**d**) Diminished cell-

surface co-localization of FRRS1L and GluR1 in patient cell lines by total internal reflection fluorescence (TIRF) microscopy. (**e**) *FRRS1L* knockdown neuronally differentiated SH-SY5Y cells show decreased Ca^{2+} influx after stimulation with 100µM AMPA (representative tracing). (**f**) Mean Ca^{2+} influx is significantly decreased by *FRRS1L* knockdown (mean ± SEM; n = 30-50 cells per condition; * p<0.05). (**g**) Bath applied 100µM AMPA-induced inward currents in control and *siFRRS1L* cells at holding potential = -80mV (representative tracings). (**h**) Current-voltage (I-V) curves under these conditions. (**i**) Mean current intensity at -80mV (mean ± SEM; n = 8-10 recordings per condition; * p<0.05).

Figure 2: *Frrs1l* deficiency leads to impairment of movement and early demise in mice. (a) Grip strength of *Frrs1l* $^{tm1b}/^{tm1b}$ is significantly reduced (p<0.0001) when compared to C57BL/6NTac controls. Measurements are an average of 3 determinations of force (g) over all 4 limbs. n = 16 C57BL/6NTac; n = 16 *Frrs1l* ^{tm1b}/+; n = 12 *Frrs1l tm1*b/*tm1b*. (b) Total distance moved in the first five minutes spent in an open field arena is significantly increased (p<0.0001) in *Frrs1l* $^{tm1b}/^{tm1b}$ when compared to C57BL6/6NTac controls. n = 20 C57BL/6NTac; n = 16 *Frrs1l* $^{tm1b}/^{+}$; n = 14 *Frrs1l* $^{tm1b}/^{tm1b}$. Error bars represent SEM for both graphs. (c) General activity in a viewing jar over a five minute period is increased in *Frrs1l* $^{tm1b}/^{tm1b}$ compared to C57BL/6NTac controls (p<0.001). *Frrs1l* $^{tm1b}/^{tm1b}$ show increased incidence of abnormal gait (p<0.0001) (d), trunk curling (e) and hindlimb grasping (p<0.0001) (f) when compared to C57BL/6NTac controls and *Frrs1l* $^{tm1b}/^{+}$ littermates. n = 20 C57BL/6NTac; n = 16 *Frrs1l* $^{tm1b}/^{+}$; n = 14 *Frrs1l* $^{tm1b}/^{tm1b}$. All data is for males and females combined, as no sex differences were observed.

Supplemental material

Supplemental Figure 1: Families with neurodegeneration, chorea, and progressive cerebral volume loss. (**a**) A total of 8 patients from 4 unrelated families were affected by this progressive neurological disease. (**b**) Diffuse cortical and cerebellar volume loss is seen by brain MRI (long arrows), with *ex vacuo* ventriculomegaly and flattening of the heads of the caudate nuclei (arrows) and periventricular fluid attenuation inversion recovery (FLAIR) hyperintense signal (arrowheads).

Supplemental Figure 2: *Frrs1l* expression pattern. (**a**) Murine *Frrs1l* expression detected by lacZ reporter at times indicated. *Frrs1l* is expressed throughout the adult brain, predominantly in cerebellum (a), differentially throughout layers of the cortex (b), thalamus (c), hippocampus (d) substantia nigra (e) and anterior olfactory nucleus (f). There is expression in the dorsal horn of the lumbar spinal cord (g), and the trigeminal ganglion (h). Outside of the nervous system, *Frrs1l* is expressed in the testis and epididymis (i) and seminiferous tubules (j). During development (E12.5) *Frrs1l* is expressed in the ventral forebrain (k) and weakly in the spinal cord (l). (**b**) RT-PCR shows similar amounts of *FRRS1L* transcript in both c.961C>T and c.845G>A patient cells when compared to controls (representative image from n = 3 experiments).

Supplemental Figure 3: Immunofluorescence studies in patients and controls. (**a**) Mutant FRRS1L did not mislocalize to alternate intracellular compartments. (**b**) FRRS1L patient fibroblasts do show diminished cell surface localization of the protein by total internal reflection fluorescence microscopy (TIRF) (representative images from 3-5 experiments per condition).

Supplemental Figure 4: *FRRS1L* knockdown in SH-SY5Y cells. FRRS1L protein levels relative to control are similar to those seen in patient fibroblasts (n = 3); transient receptor potential channel 1 and actin serve as loading controls.

Supplemental Figure 5: Construction and validation of the *Frrs1l* ^{tm1b}/^{tm1b} mouse. (**a**) Schematic depicting the construction of the *Frrs1l* null mouse using a knockout-first-reporter tagged insertion allele vector (www.i-dcc.org/imits/targ_rep/alleles/14093/vector-image) (**b**) Sequence alignment based on Sanger sequencing verifying effective loss of exon 3 (www.i-dcc.org/imits/targ_rep/alleles/14093/targeting-vector-genbank-file). (**c**) Southern blot for *FRRS1L-TM1A* showing expected bands indicating that the 5' (12.6kb; Mfel) and 3' (19.2kb; BstE11) ends of the construct, respectively, are correctly positioned and intact. (**d**) Immunoblot depicting dose-response of Frrs1l protein levels in wild-type, heterozygous and homozygous animals (representative image).

Supplemental Figure 6: Neuropathological analysis of Frrs1l knockout mice. Hematoxylin & eosin stain shows normal cortical, basal ganglia and cerebellar architecture without evidence of cortical atrophy (representative images).

Supplemental Table 1. Clinical features of *FRRS1L* patients

Supplemental Table 2. Regions of homozygosity shared by index family members

Supplemental Table 3. Sequence variants identified in a cohort of Huntington disease-like patients lacking triplet repeat expansions in HTT

Supplementary Table 4. Survival of wild-type vs. *Frrs1l* ^{tm1b}/^{tm1b} mice

Supplemental Video 1: Affected patient from family 2 demonstrating generalized chorea

Supplemental Video 2: *Frrs1l* ^{tm1b}/^{tm1b} mice exhibit abnormal hyperkinetic movements (a) compared to wild-type controls (b)

Patients The index family hailed from southern Saudi Arabia. The parents were distant cousins. All five of the couple's children developed progressive chorea, dementia and epilepsy. One child (patient 1_II-2) had already succumbed to the disease at the time of ascertainment. All children were born at term without complications. All had normal early development, but began to regress between the ages of 18-22 months, ceasing to walk and losing expressive language. This coincided with the onset of hemiclonic and tonic-clonic seizures with some response to carbamazepine and/or valproate. Examinations disclosed no dysmorphic features, normal fundi, global developmental delay, diffuse hypotonia, and generalized chorea with a paucity of volitional movement. All of the affected children became less responsive to the environment over time, and their hyperkinetic movement disorder gradually gave way to a rigid, akinetic state in late adolescence.

Patient 2_II-1, an unrelated girl, was born to non-consanguineous Caucasian parents after an unremarkable pregnancy at 31 weeks gestation. At 4 months of age, she started having choreoathetotic movements of her hands, opisthotonic posturing and occasional hand tremors. She gained developmental motor and language milestones until age 13 months, when she began to have generalized tonic-clonic seizures. During periods of illness, her seizures were accompanied by chaotic eye movements and forced gaze deviation, frequent episodes of loss of tone, fluctuating levels of alertness, and truncal hypotonia. Between 14 and 27 months of age, her seizures remained refractory to levetiracetam, phenobarbital, clobazam and the ketogenic diet. This was associated with developmental regression. Her examination was significant for generalized chorea and ballism (Video 1).

Patient 3_II-1 was a Puerto Rican girl with no recognized consanguinity born at 37 weeks estimated gestational age. She cruised with an ataxic gait beginning at 11 months and used several words appropriately before experiencing a neurodevelopmental regression at age 24 months. She developed juvenile spasms and was later diagnosed with Lennox-Gastaut syndrome. She initially benefited from the ketogenic diet, but her seizures were never fully controlled. Examination revealed horizontal and vertical nystagmus with esotropia, generalized chorea and cogwheel rigidity of her upper limbs, hyperreflexia, hypotonia, and diminished volitional movement (she did not reach purposefully or have a means of locomotion). No expressive language was evident.

Patient 4_II-1, an unrelated girl, was born at term by caesarean section to consanguineous Moroccan parents after a pregnancy complicated by gestational diabetes. Poor muscle tone was noted from early infancy, and she has never attained good head control. She was delayed in reaching early motor milestones. At age 10 months, she could fix and follow objects, albeit with saccadic pursuit, and could grasp nearby objects and bring them to her mouth. She demonstrated choreoathetoid movements of her arms and hands. Her alertness fluctuated, putatively related to hypomotor seizures. These proved resistant to levetiracetam, valproic acid and vigabatrin, and her eye contact and muscle tone deteriorated. At age 17 months, she was admitted with status epilepticus. Phenobarbital led to satisfactory seizure control, and she has now mainly short, multifocal clonic seizures and intermittent myoclonus. She is currently fed via nasogastric tube.

Homozygosity mapping & parametric linkage analysis Genomic DNA was extracted from whole blood, and regions of homozygosity shared by affected individuals but absent in unaffected individuals in family 1 were identified using Affymetrix Whole-Genome CytoScan® HD single nucleotide polymorphism (SNP) arrays according to the manufacturer's instructions. MERLIN was used to calculate LOD scores.

Exome analysis Exonic targets were enriched with the SeqCap EZ Human Exome Library v3.0 kit (Nimblegen) and sequencing was performed on an Illumina HiSeq2000 or 2500 according to the manufacturer's instructions in order to generate paired-end reads. Average coverage depth was >70× within the targeted exome. Sequencing reads were aligned to the NCBI human reference genome (GRCh37/hg19) using the Burrow-Wheeler Aligner (BWA 0.7.10). Picard Tools (1.111) was subsequently used for sorting and marking duplicates. Local realignment, base quality score recalibration, and variant calling was performed using the Genome Analysis Toolkit (GATK 3.3-0) and variant call files were evaluated using NextCode (Cambridge, MA) or Cartagenia Bench Lab NGS software (Cambridge, MA). Filtering was performed by removing low-quality calls (Illumina threshold <20) and excluding variants with an MAF >0.01 based on the ExAc Browser and Exome Variant Server databases while prioritizing homozygous variants predicted deleterious by SIFT, Polyphen-2, MutationTaster and CADD.

Sanger sequence analysis Variants identified by whole exome sequencing were confirmed by Sanger sequencing. Primers (sequences available upon request) were designed to span intron-exon boundaries of NM_014334.

Cells Primary fibroblast lines were established from 3mm circular punch biopsies and confirmed mycoplasma-free. Patient and age-matched control cells of equivalent early passage number were grown in Dulbecco's modified Eagle's medium (DMEM; ThermoFisher), supplemented with 10% (v/v) fetal calf serum, 2 mM L-glutamine, 50 U/ml penicillin and 50 µg/ml streptomycin. SH-SY5Y cells were obtained from the American Type Culture Collection (Manassas, VA), cultured in DMEM, and neuronally differentiated by growth in DMEM + 10µM retinoic acid for 7 days.

Antibodies Antibodies included anti-FRSS1L (Atlas, 1:1000 for WB and 1:100 for IF), anti-Na/K ATPase (Abcam, 1:100 for IF), anti-GM130 (BD Biosciences, 1:100 IF), anti-EEA1 (Sigma, 1:100 IF), and anti-GluR1 (Cell Signaling, 1:100 for IF), anti-calnexin (Abcam, 1:100 for IF), anti-TRPC1 (Alomone labs, 1:500 WB); anti-β-actin (Santa Cruz Biotechnology, 1:1000 WB).

Transfections SH-SY5Y cells ($1.5x10^5$ cells/ml) were transfected with FRRS1L siRNA or scrambled control siRNA (Ambion) using RNAiMax reagent (Ambion).

Calcium Measurements Neuronally-differentiated SH-SY5Y **c**ells were incubated with 2 µM fura-2 (Molecular Probes) for 45 min and washed twice with Ca^{2+}-free standard external solution (10 mM HEPES, 120 mM NaCl, 5.4 mM KCl, 1 mM $MgCl_2$, 10 mM glucose, pH 7.4). Fluorescence intensity of Fura-2-loaded cells was monitored with a CCD camera-based imaging system and analyzed using PCI software (Compix, Cranberry, PA), to provide ratios of Fura-2 fluorescence at 340 nm excitation to that of 380 nm excitation (F340/F380).

Electrophysiology For patch clamp experiments, coverslips with neuronally-differentiated SH-SY5Y cells were perfused with Ringer's solution (145mM NaCl, 5mM KCl, 1mM $MgCl_2$, 1mM $CaCl_2$, 1 µM tetrodotoxin (TTX), 10mM HEPES, 10mM Glucose, pH 7.3). Whole cell currents were recorded using an Axopatch 200B (Molecular Devices, Sunnyvale, CA) and a patch pipette filled with standard intracellular solution (145 mM CsCl, 0.1 mM $CaCl_2$, 2 mM $MgCl_2$, 1 mM, EGTA, and 5 mM HEPES, pH 7.2). With holding potential = -60mV, voltage ramps ranging from -100mV to +100mV and 100ms duration were delivered at 2s intervals after whole cell configuration was formed. Basal leak was subtracted from final currents.

Microscopy Patient-derived fibroblasts and controls were grown to near-confluence, washed twice, fixed in 4% paraformaldehyde, permeabilized with PBS/0.1% Triton X-100 and labeled

with primary antibody and visualized with secondary antibody. Cells were visualized using the 100X objective of an A1 confocal microscope (Nikon, Melville, NY) equipped with an Andor iXon 897 (Andor Technologies Ltd., Belfast, UK) for total internal reflection fluorescence (TIRF) imaging.

Immunoblotting Cell contents were released using lysis buffer (25mM Tris-HCl pH 7.6, 150mM NaCl, 1% NP-40, 1% sodium deoxycholate, 0.1% SDS, and Roche complete protease inhibitor). Protein concentration was determined by BCA assay (Pierce). Protein extracts were separated by 12% SDS-PAGE under reducing conditions, transferred to PVDF membranes and probed with primary antibodies.

Mice All experiments were performed under license from the UK Home Office (30/2890) and local Animal Welfare and Ethical Review Body approval. All animals were bred and maintained on site. The *Frrs1l* $^{tm1b(EUCOMM)Hmgu}$ mice were generated at MRC Harwell which distributes these mice on behalf of the European Mouse Mutant Archive (www.infrafrontier.eu) using the knockout first method (1, 2, 3). Funding and associated primary phenotypic information may be found at www.mousephenotype.org. Mice were housed on a 12:12 light dark cycle with free access to water and fed ad libitum with RM3 (SDS). *Frrs1 l* $^{tm1a(EUCOMM)Hmgu}$ mice were derived from C57BL6/NTac ES cells. The null allele, *Frrs1l* $^{tm1b(EUCOMM)Hmgu}$, was created by carrying out an IVF using *Frrs1l* $^{tm1a/+}$ sperm and C57BL6/NTac oocytes. Soluble cell permeable cre (TAT-Cre (Tat-NLS-Cre, HTNC, HTNCre), Excellegen, Rockville, USA) was added to two cell *Frrs1l* $^{tm1a/+}$ embryos to convert them to *Frrs1l* $^{tm1b/+}$. The addition of cre excised the selection cassette and exon 3 of the *Frrs1l* gene, creating a lacZ tagged null allele. Following washing to remove soluble cre, the IVF procedure was completed. The *Frrs1l* $^{tm1b/+}$ offspring were crossed to C57BL/6NTac and then intercrossed to create *Frrs1l* $^{tm1b/+}$and *Frrs1l* $^{tm1b/tm1b}$.

Open field Mice were placed in square arenas made of grey perspex (44x44cm) at lux of 150-200. Mice were allowed to explore the arenas for 20 minutes whilst tracking was recorded by Ethovision XT software (Noldus, Netherlands). Arenas were divided into periphery and center zones and parameters such as time moving, distance moved and duration in zone were calculated. For a full list of parameters see https://www.mousephenotype.org/impress/protocol/81/7.

Grip strength Mice were held by their tail and placed on a grip strength apparatus (Bioseb, France) before being pulled down the grid and grip strength recorded. Each mouse completed three trials for forepaws and three trials for combined fore and hindpaws. Data across the three trials were averaged.

Combined SHIRPA and dysmorphology Mice were observed for behavioral changes using a modified SHIRPA protocol (4). Briefly, mice were placed on a wire grid in a viewing jar (height 15 cm, diameter 11 cm), where they were observed for five minutes for general activity and behavior. Mice were then transferred to an arena (55 x 33cm) for observations of motor behaviors. Finally mice were handled to detect phenotypes including dysmorphic abnormalities, trunk curling and limb grasping. A full list of parameters can be found at https://www.mousephenotype.org/impress/protocol/186/7.

Statistical analysis Continuous data was analyzed using Students t-test while categorical data was analyzed using Fisher's exact test. A chi squared test was carried out to determine the significance of deviation from normal Mendelian ratios. Statistical analysis was carried out using GraphPad Prism 6 and R version 3.2.2 and R Studio version 0.99.485 and the following conventions were used: * $p \leq 0.05$; ** $p \leq 0.01$; *** $p \leq 0.001$; **** $p \leq 0.0001$.

Reference

1) Pettitt SJ, Liang Q, Rairdan XY, Moran JL, Prosser HM, Beier DR, Lloyd KC, Bradley A & Skarnes WC (2009) Agouti C57BL/6N embryonic stem cells for mouse genetic resources. *Nature Methods*, 6(7), 493-495.
2) Skarnes, W.C., Rosen, B., West, A.P., Koutsourakis, M., Bushell, W., Iyer, V., Mujica, A.O., Thomas, M., Harrow, J., Cox, T. et al. (2011) A conditional knockout resource for the genome-wide study of mouse gene function. *Nature*, 474, 337-342.
3) Bradley A, Anastassiadis K, Ayadi A, Battey JF, Bell C, Birling M-C, Bottomley J, Brown SD, Bürger A, Bult CJ, Bushell W, Collins FS, Desaintes C, Doe B, Economides A, Eppig JT, Finnell RH, Fletcher C, Fray M, Frendewey D, et al. (2012) The mammalian gene function resource: the international knockout mouse consortium. *Mamm. Genome*, 23(9-10), 580-586.
4) Rogers DC, Peters J, Martin JE, Ball S, Nicholson SJ, Witherden AS, Hafezparast M, Latcham J, Robinson TL, Quilter CA, Fisher EM. SHIRPA, a protocol for behavioral assessment: validation for longitudinal study of neurological dysfunction in mice. *Neurosci Lett.* 2001 Jun 22;306(1-2):89-92.

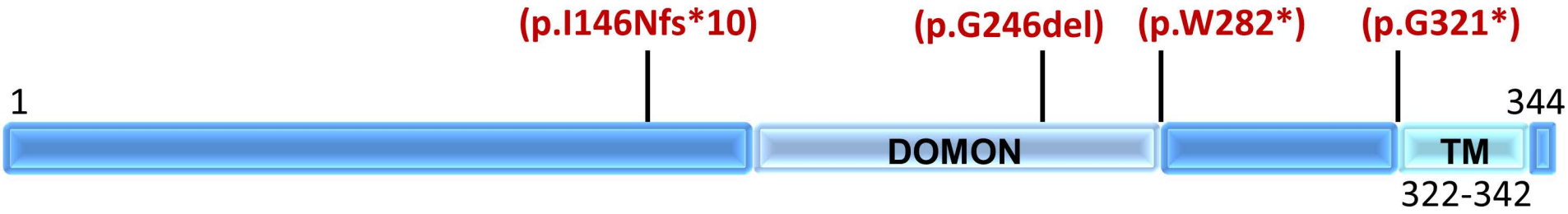
(p.I146Nfs*10)
(p.G246del)
(p.W282*)
(p.G321*)
1
344
DOMON
TM
322-342

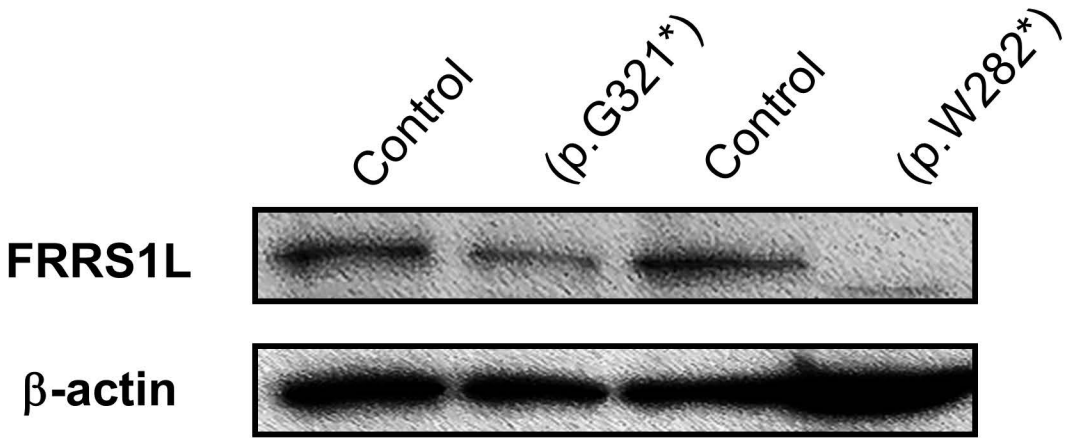
Control
(p.G321*)
Control
(p.W282*)
FRRS1L
β-actin

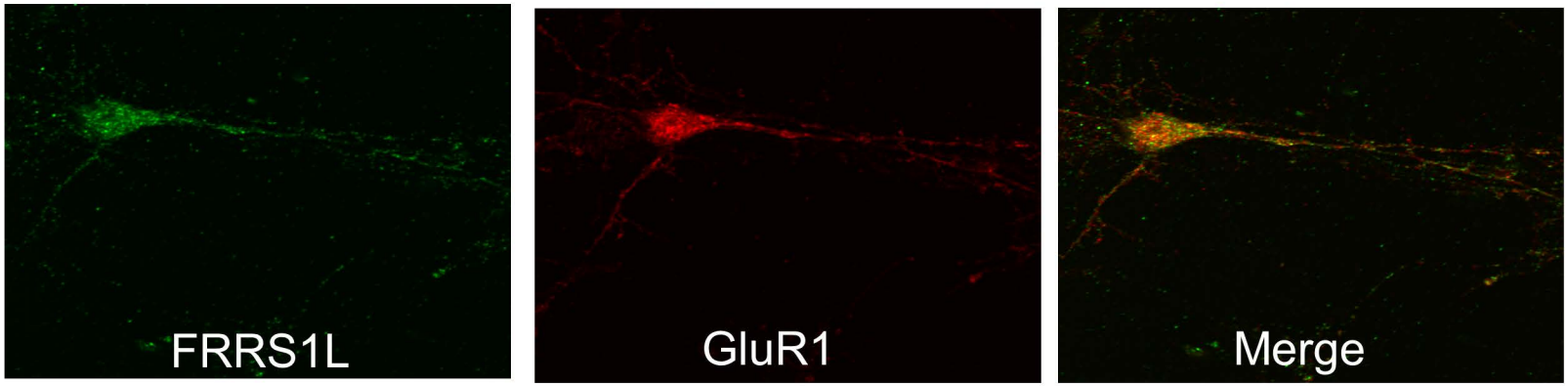
FRRS1L
GluR1
Merge

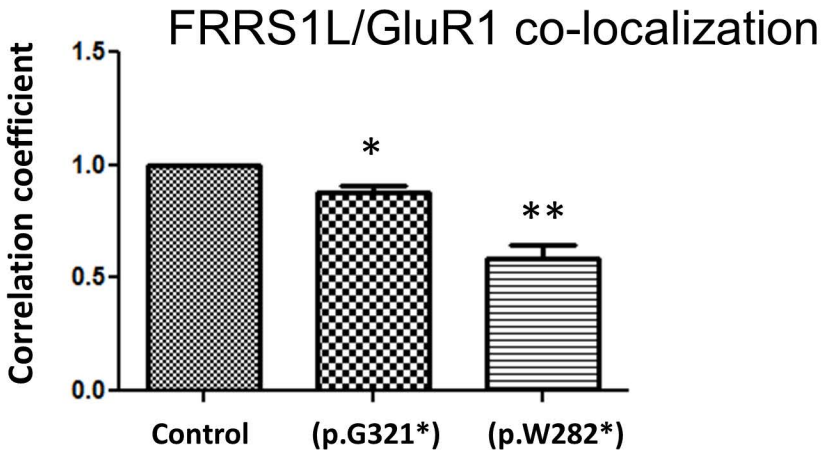
FRRS1L/GluR1 co-localization
Correlation coefficient
1.5
1.0
0.5
0.0
*
**
Control
(p.G321*)
(p.W282*)

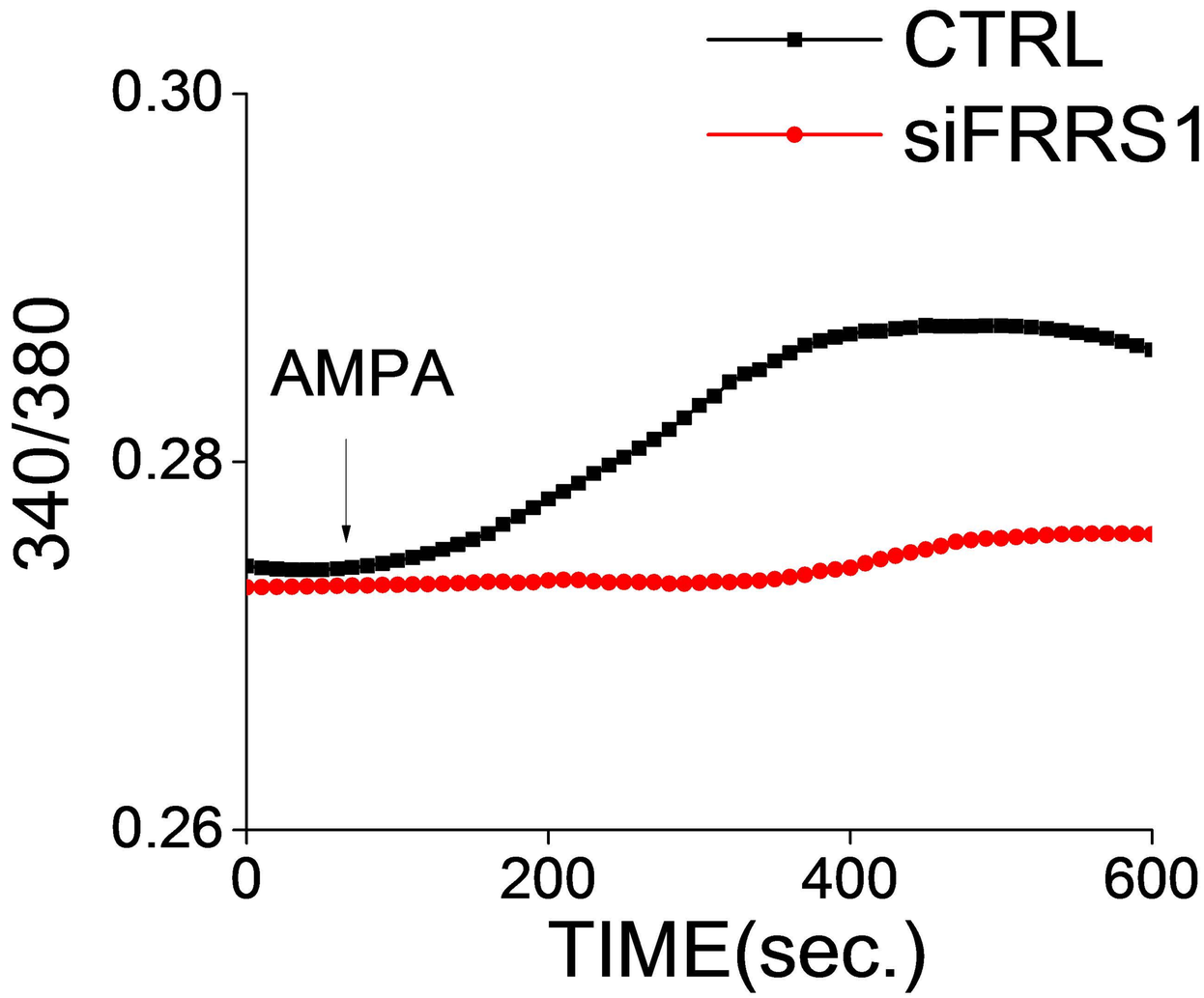
CTRL
siFRRS1L
0.30
0.28
0.26
340/380
AMPA
0
200
400
600
TIME(sec.)

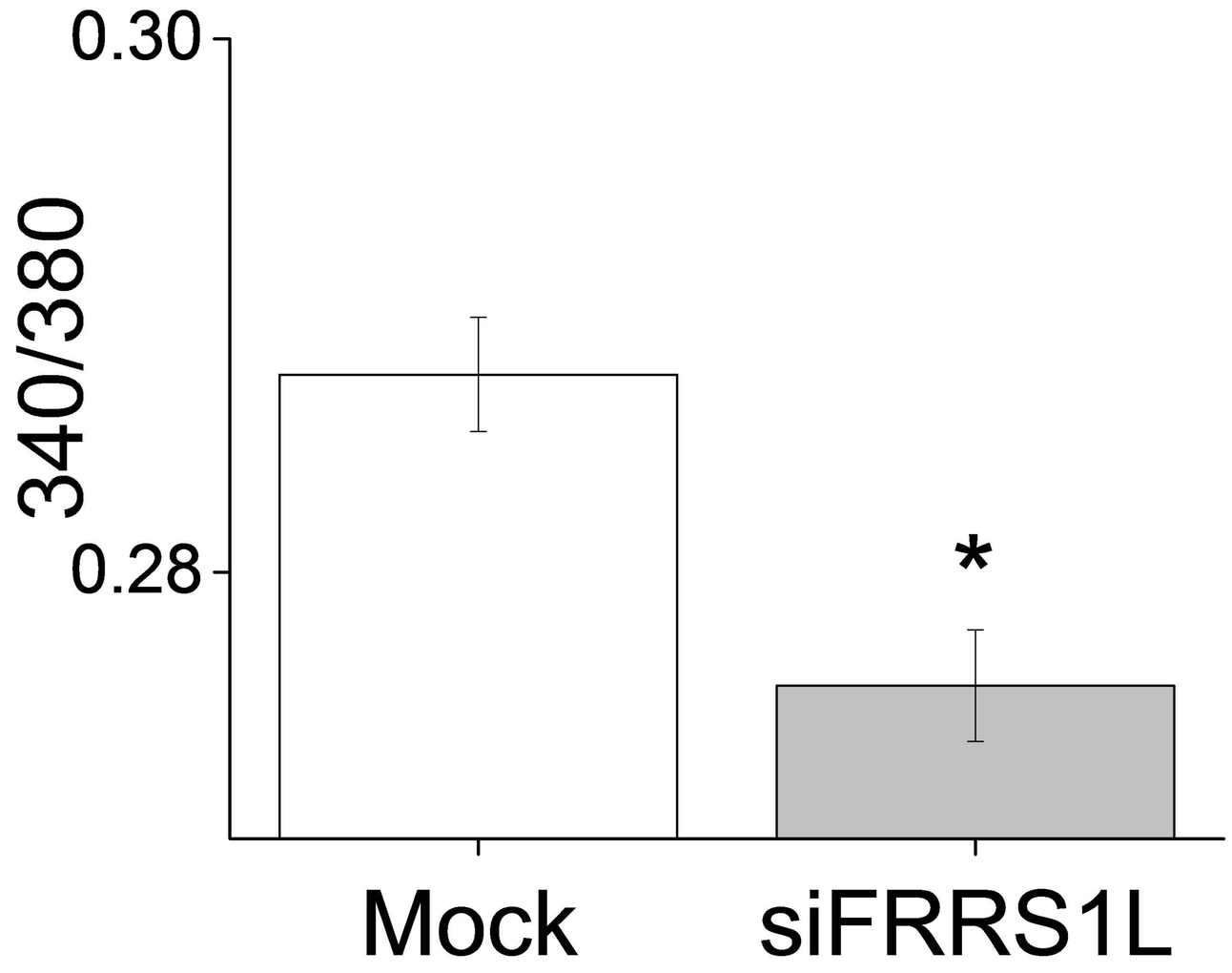
0.30
340/380
0.28
*
Mock
siFRRS1L

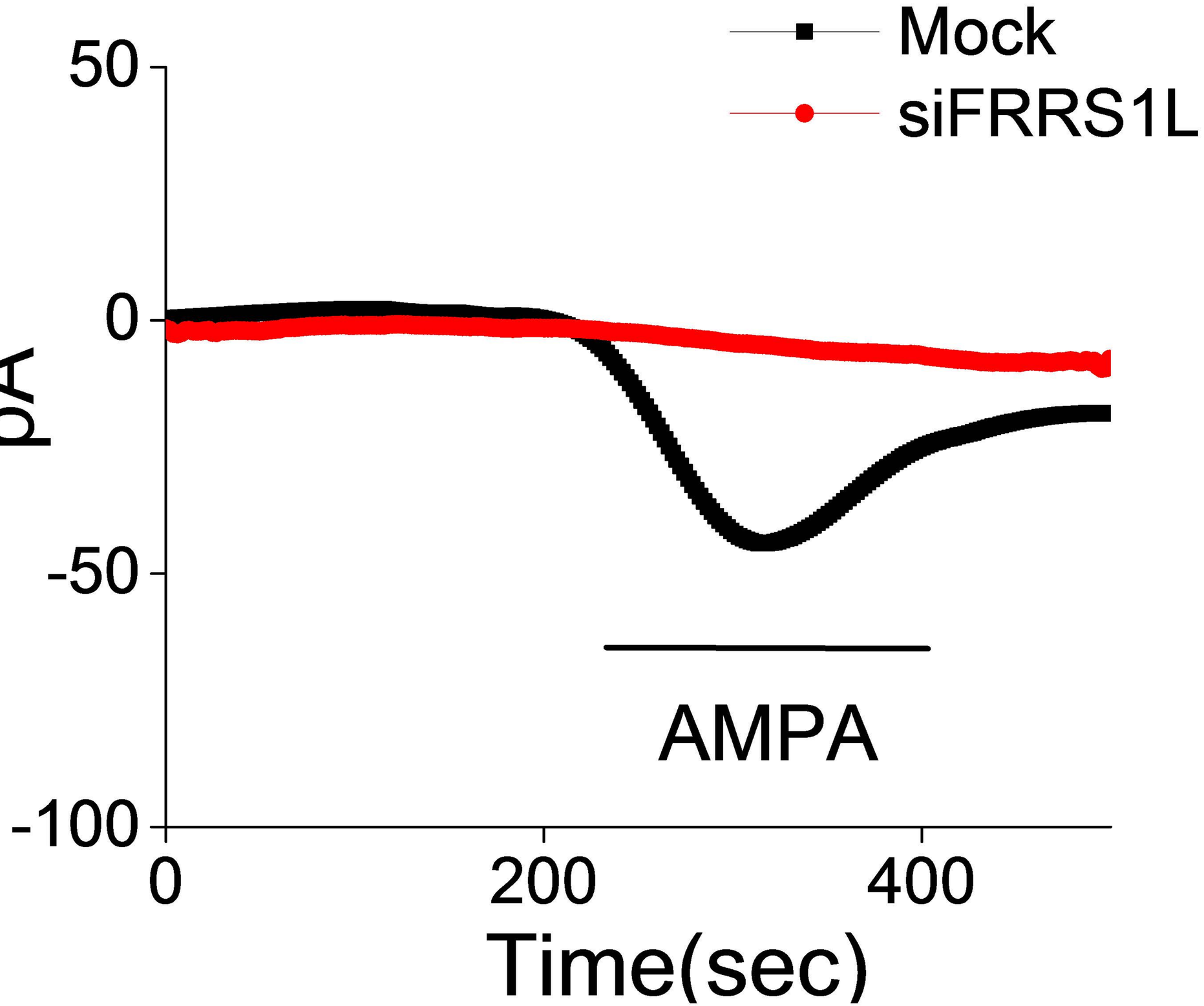
Mock
siFRRS1L
50
0
-50
-100
pA
AMPA
0
200
400
Time(sec)

Current-voltage (I-V) curves

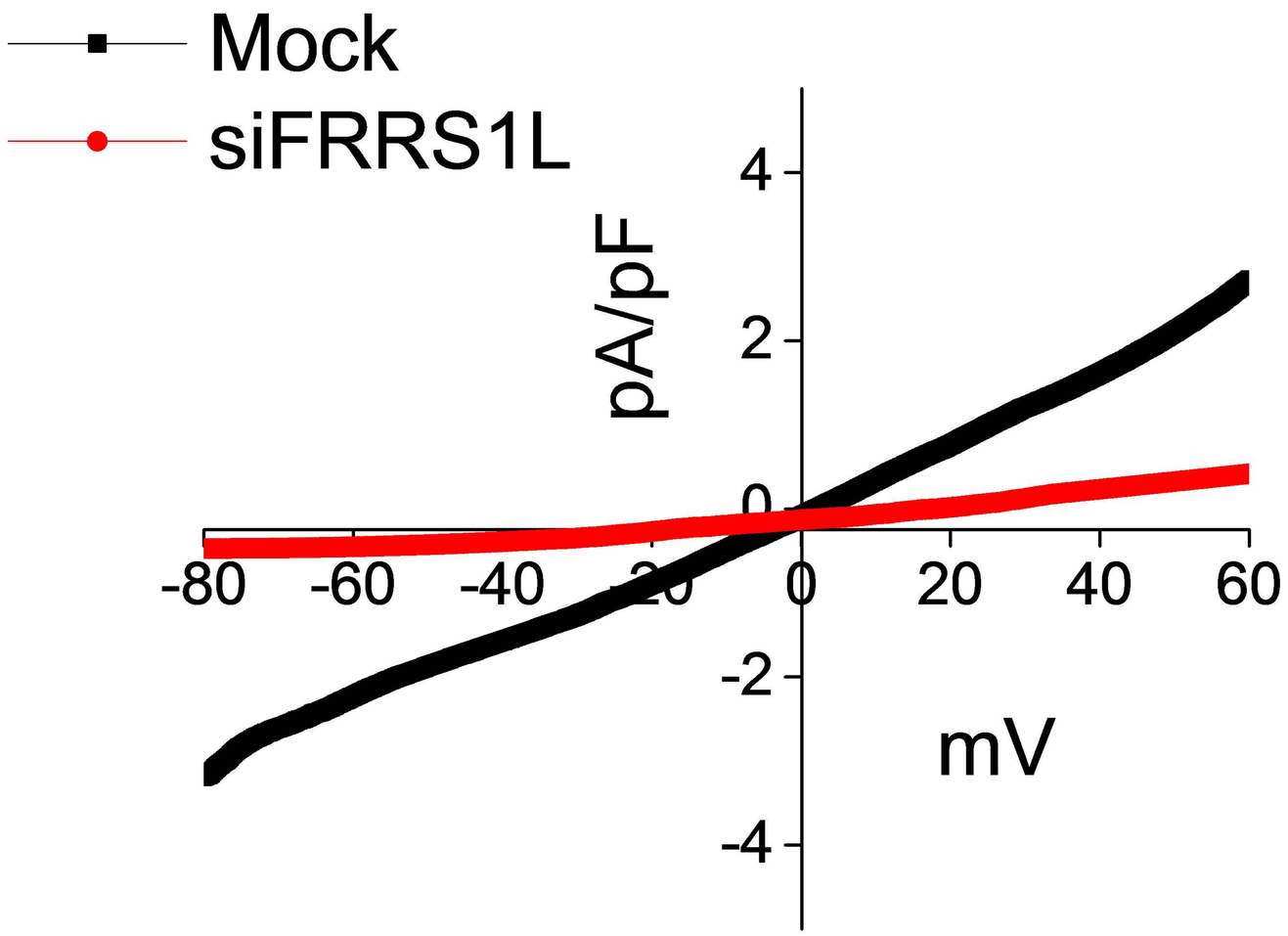

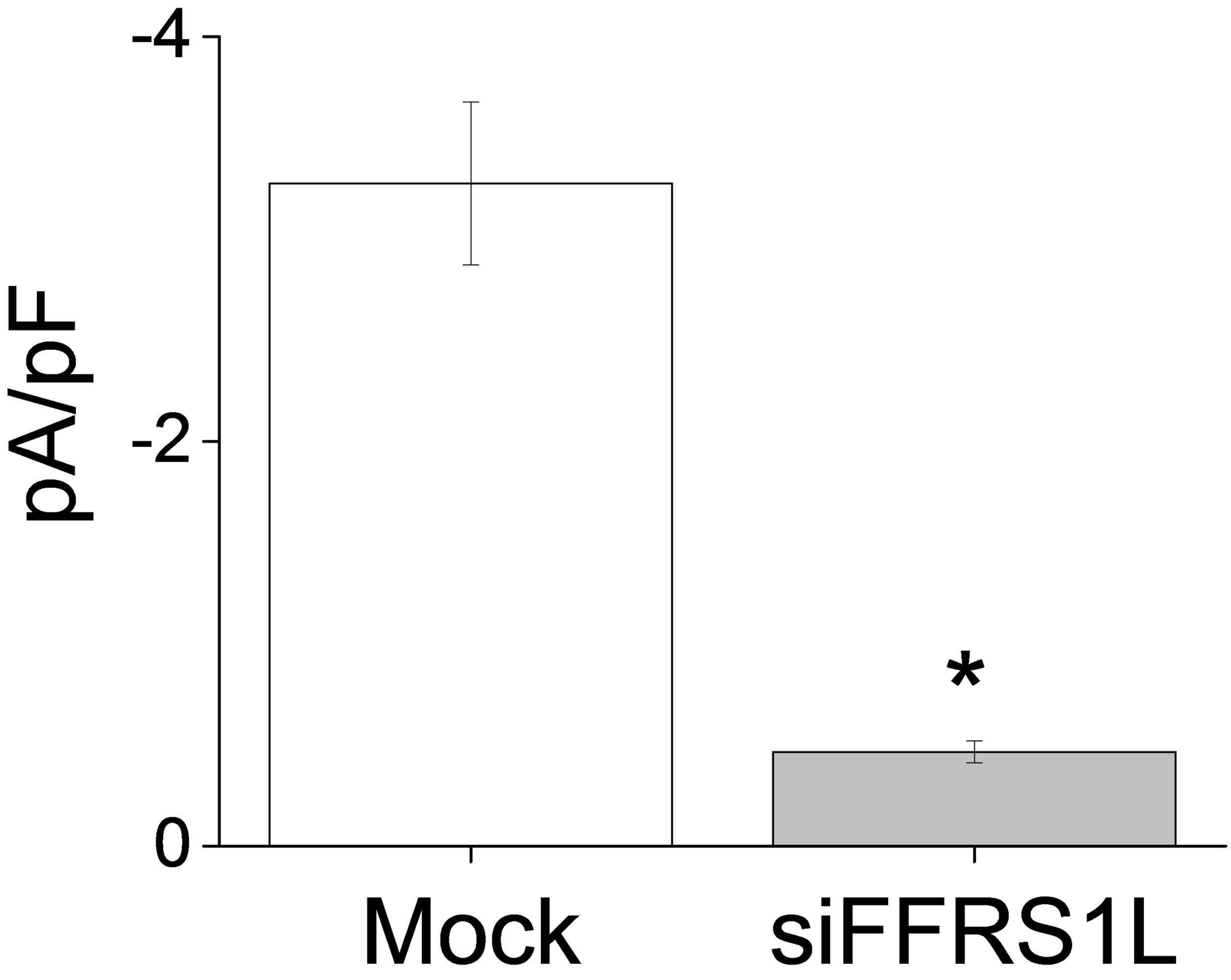
-4
-2
0
pA/pF
*
Mock
siFFRS1L

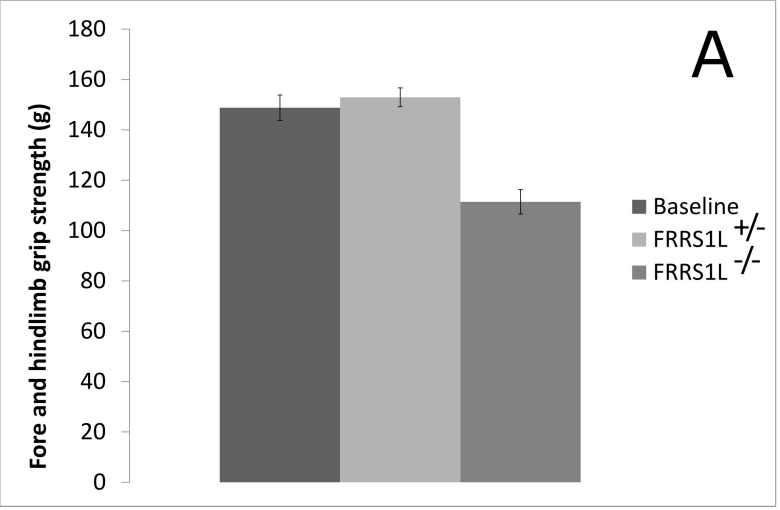
A
Fore and hindlimb grip strength (g)
180
160
140
120
100
80
60
40
20
0
Baseline
FRRS1L +/-
FRRS1L -/-

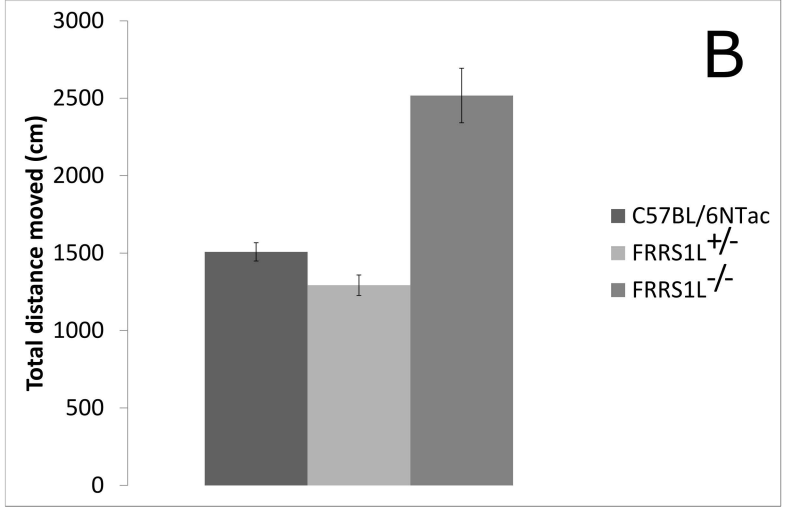
B
Total distance moved (cm)
3000
2500
2000
1500
1000
500
0
C57BL/6NTac
FRRS1L+/-
FRRS1L-/-

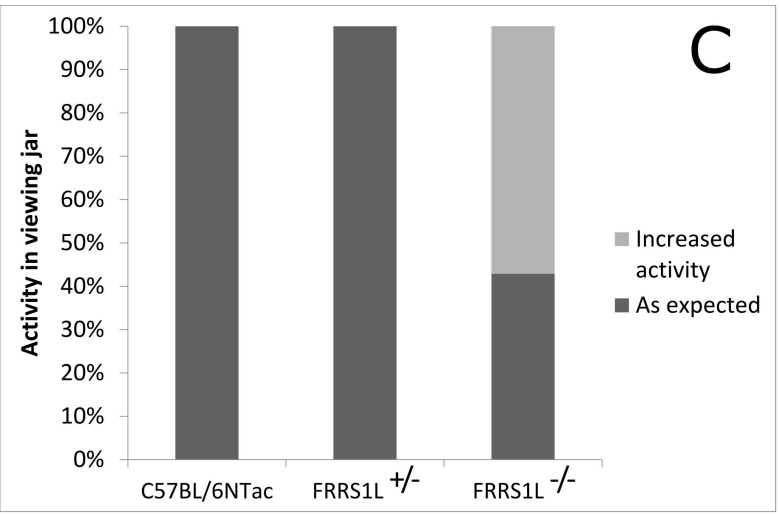
C
Activity in viewing jar
100%
90%
80%
70%
60%
50%
40%
30%
20%
10%
0%
Increased activity
As expected
C57BL/6NTac
FRRS1L +/-
FRRS1L -/-

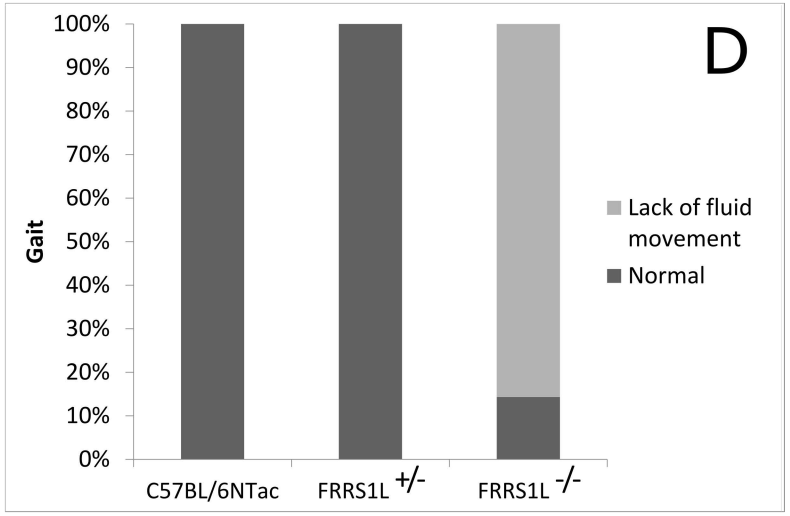
D
Gait
100%
90%
80%
70%
60%
50%
40%
30%
20%
10%
0%
Lack of fluid movement
Normal
C57BL/6NTac
FRRS1L +/-
FRRS1L -/-

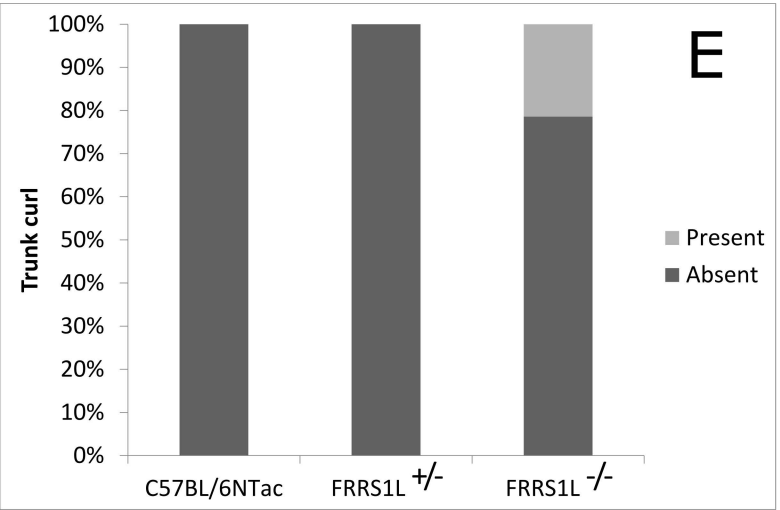
E
Trunk curl
100%
90%
80%
70%
60%
50%
40%
30%
20%
10%
0%
Present
Absent
C57BL/6NTac
FRRS1L +/-
FRRS1L -/-

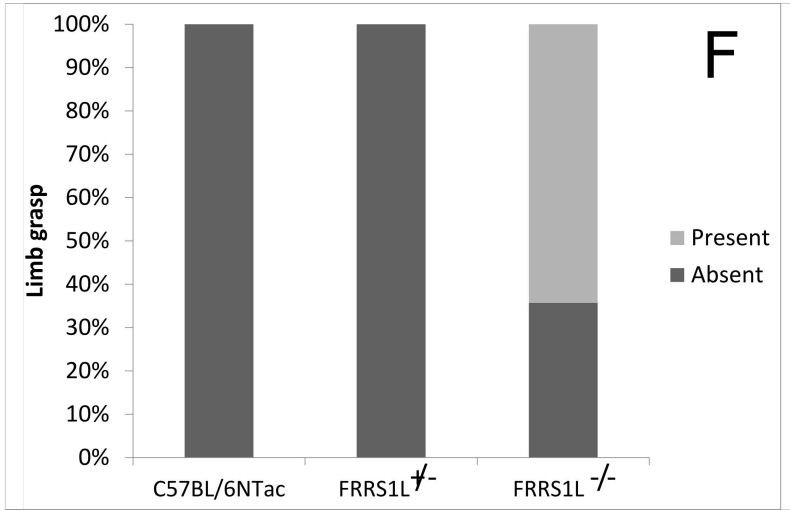
F
Limb grasp
100%
90%
80%
70%
60%
50%
40%
30%
20%
10%
0%
Present
Absent
C57BL/6NTac
FRRS1L +/-
FRRS1L -/-

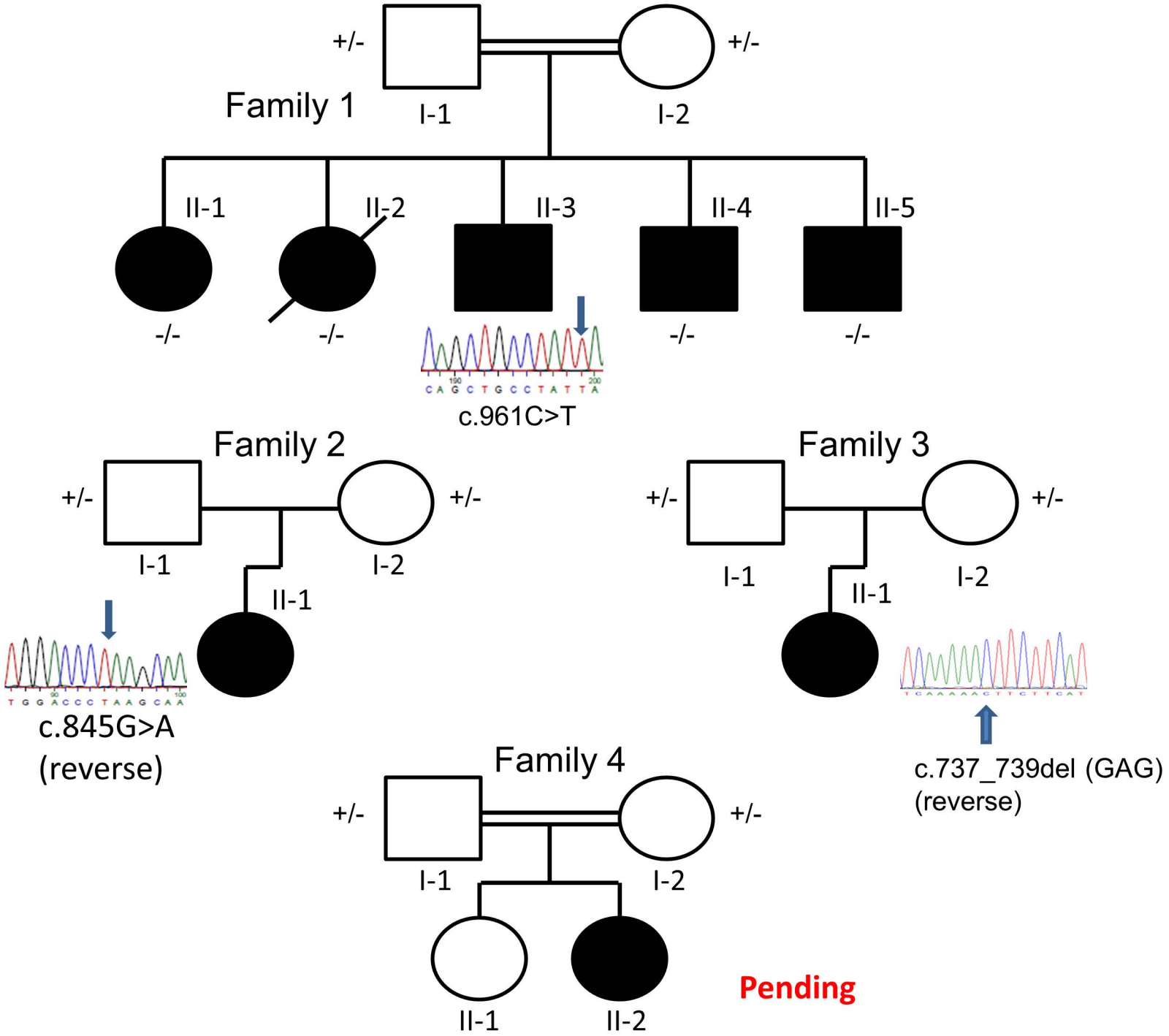
Family 1
+/-
+/-
I-1
I-2
II-1
II-2
II-3
II-4
II-5
-/-
-/-
-/-
-/-
c.961C>T
Family 2
+/-
+/-
I-1
I-2
II-1
c.845G>A
(reverse)
Family 3
+/-
+/-
I-1
I-2
II-1
c.737_739del (GAG)
(reverse)
Family 4
+/-
+/-
I-1
I-2
II-1
II-2
Pending

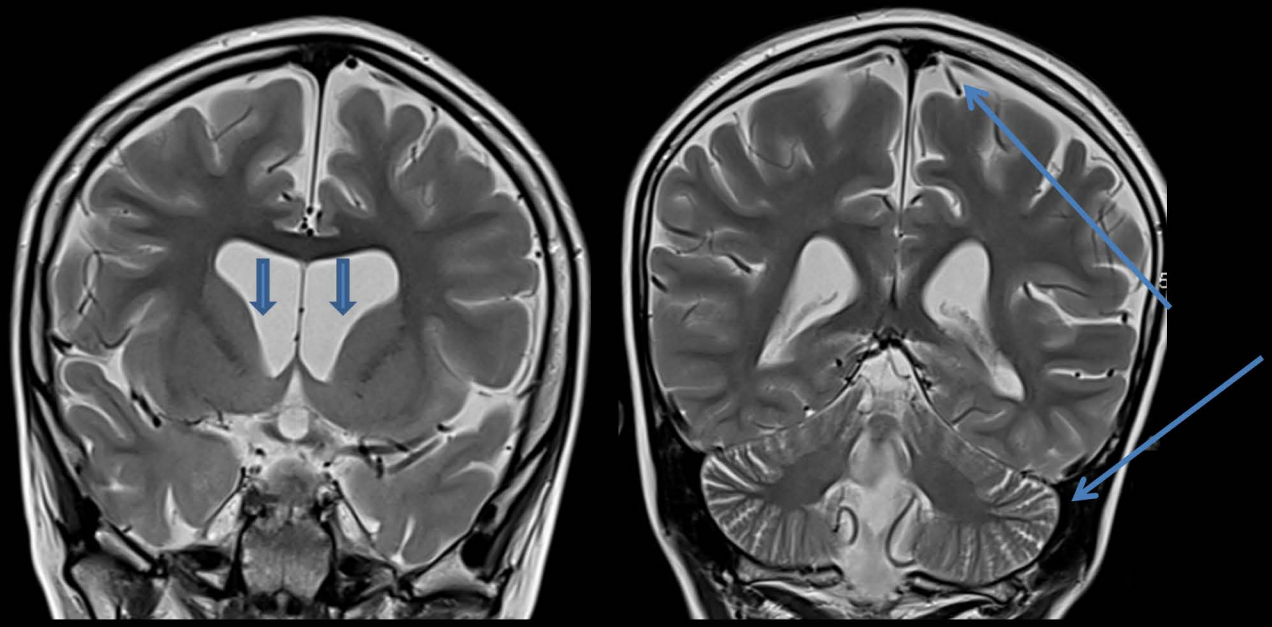

Family 1_II-3

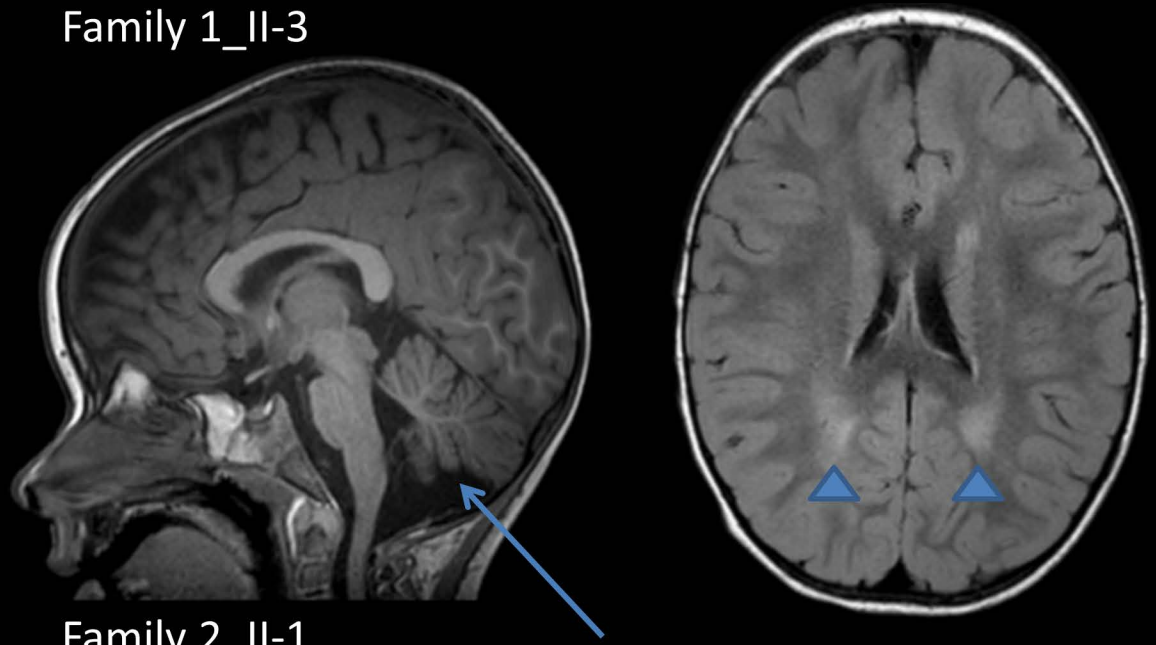

Family 2_II-1

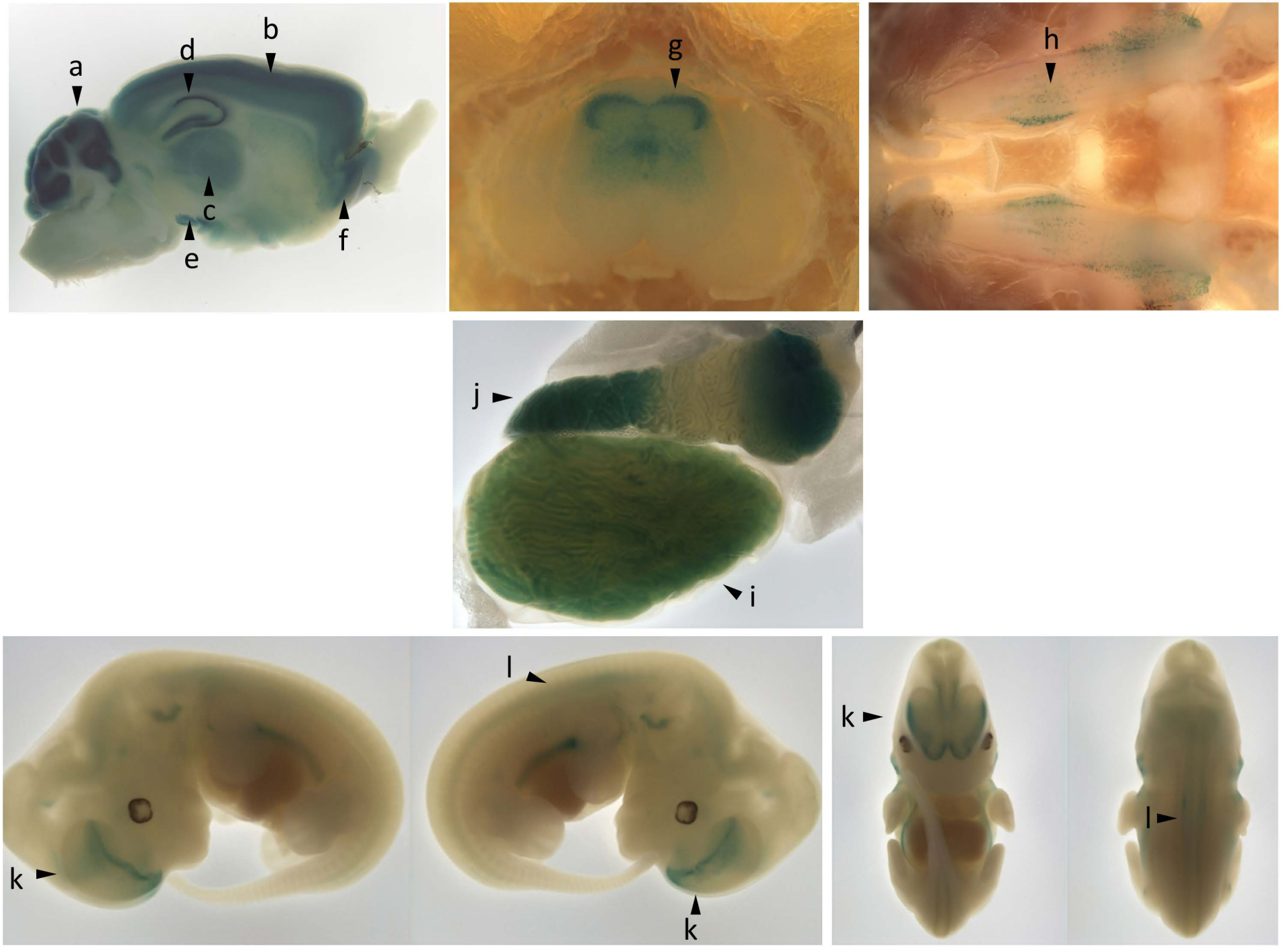
a
d
b
c
e
f
g
h
j
i
k
l
k
l
k
l

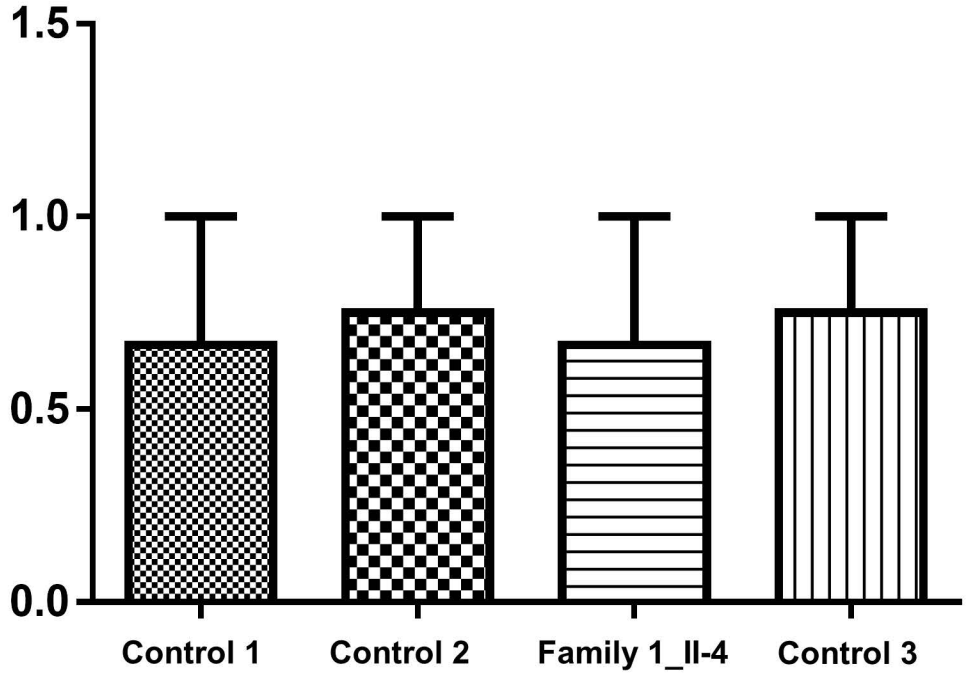
1.5
1.0
0.5
0.0
Control 1
Control 2
Family 1_II-4
Control 3

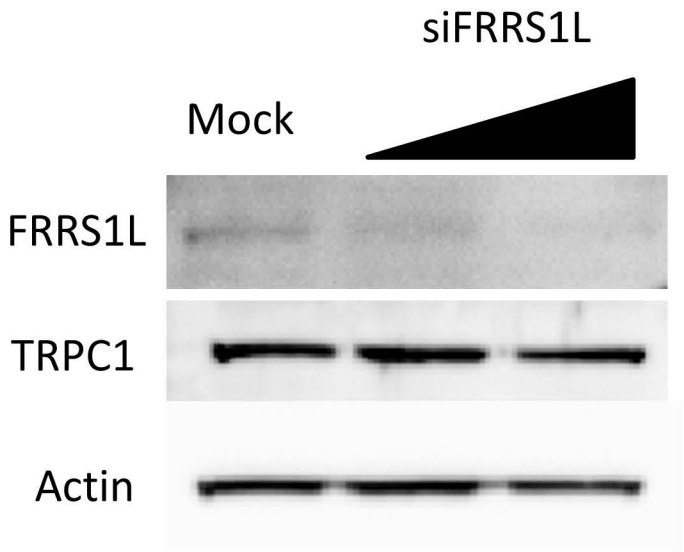
siFRRS1L
Mock
FRRS1L
TRPC1
Actin

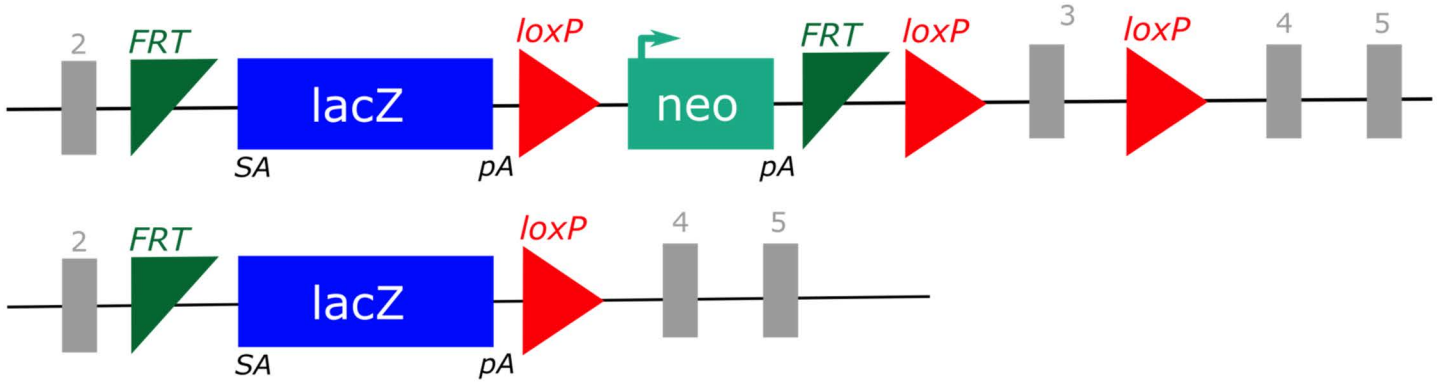
2
FRT
lacZ
loxP
neo
FRT
loxP
3
loxP
4
5
SA
pA
pA
2
FRT
lacZ
loxP
4
5
SA
pA

Alignment of LoxP PCR products (floxed region vs. reference NM_001142965)

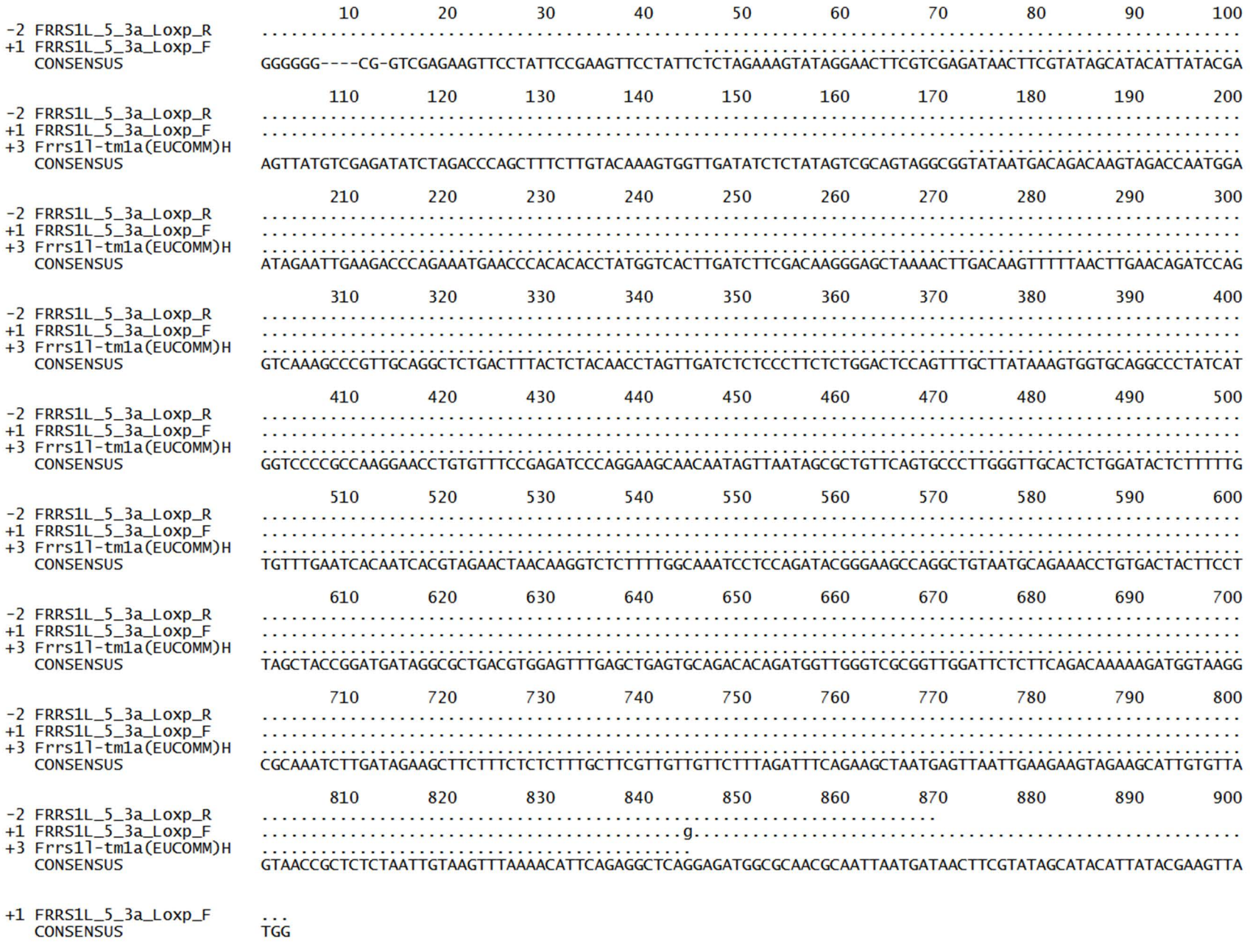

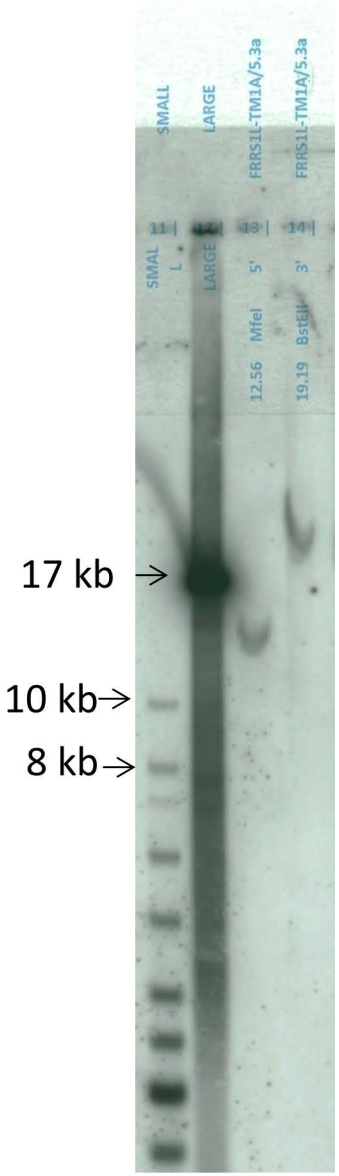
SMALL
LARGE
FRRS1L-TM1A/5.3a
FRRS1L-TM1A/5.3a
11
12
13
14
SMAL
L
LARGE
5'
3'
12.56
MfeI
19.19
BstEII
17 kb
10 kb
8 kb

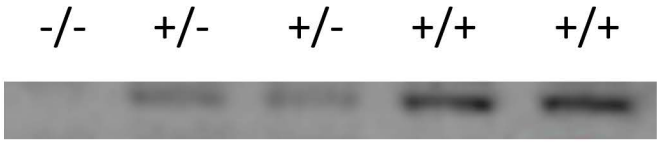

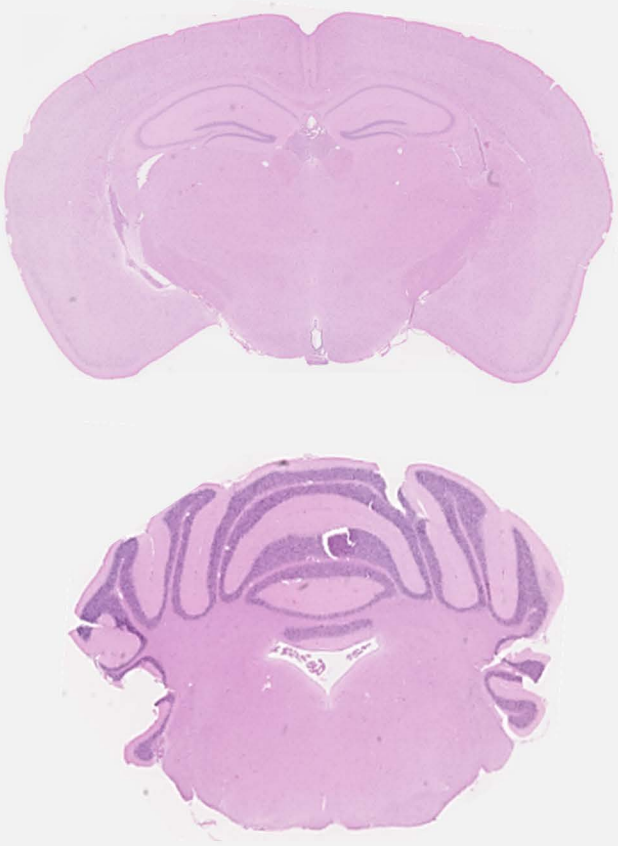

Wild-type

Frrs1l $^{-/-}$

Supplementary Table 1: Clinical features of FRRS1L patients

Patient	Mutation	Age at onset	Reg-ression	Intellectual impairment	Movement disorder	Epilepsy	Neuromotor	Other
1_II-1	(p.G321*)	18 months	Yes	Severe; no expressive speech	Chorea; later rigidity, hypokinesia	Focal	Spasticity; impaired volitional movement	
1_II-2	(p.G321*)	22 months	Yes	Severe; no expressive speech	Chorea; later rigidity, hypokinesia	Hemiclonic seizures; later generalized	Spasticity; impaired volitional movement	Died at age 16
1_II-3	(p.G321*)	22 months	Yes	Severe; no expressive speech	Chorea; later rigidity, hypokinesia	Hemiclonic seizures	Spasticity; impaired volitional movement	
1_II-4	(p.G321*)	23 months	Yes	Severe; no expressive speech	Chorea; later rigidity, hypokinesia		Spasticity; impaired volitional movement	
1_II-5	(p.G321*)	24 months	No	Severe; no expressive speech	Chorea	Hemiclonic seizures		
2_II-1	(p.W282*)	4 months	No	Severe; no expressive speech	Chorea, ballism	Multifocal; intractable	Hypotonia; impaired volitional movement	
3_II-1	(p.G246del)	24 months	Yes	Severe; no expressive speech	Chorea; cogwheel rigidity	Juvenile Spasms/ Lennox-Gastaut	Hypotonia; impaired volitional movement	Horizontal & vertical nystagmus
4_II-2	(p.Ile146Asnfs*10)			Severe; no expressive speech	Chorea; myoclonus			

Chromosome	Start	End	Size (Mb)
1	147,779,938	151,347,700	3.5
3	62,613	4,878,792	4.8
9	104,622,396	119,149,440	14.5
16	31,901,547	35,220,544	3.3
X	61,932,503	65,386,406	3.5

Rare heterozygous *FRRS1L* variants in a cohort of 202 patients with mixed movement disorders (ataxia, spastic paraplegia, dystonia, parkinsonism, etc.) and neurodegeneration

***FRRS1L* variant**	**ESP6500**	**ExAc**	**Phenotype**
c.T469A; (p.C157S)	-	8.13E-06	Ataxia, optic nerve atrophy
c.721delG; (p.A241fs)	-	8.13E-06	Multiple system atrophy
c.T686C; (p.V229A)	0.000231	7.40E-04	Ataxia
c.A885G; (p.I295M)	0.000077	1.63E-05	Multiple system atrophy

Survival at E18.5 and P21

Age	*Frrs1l* $^{+/+}$	*Frrs1l* $^{+/-}$	*Frrs1l* $^{-/-}$
E18.5	6	26	13
3 weeks	60	101	16